IEEE Access
Multidisciplinary | Rapid Review | Open Access Journal

Received 24 November 2022, accepted 11 December 2022, date of publication 15 December 2022,
date of current version 22 December 2022.

Digital Object Identifier 10.1109/ACCESS.2022.3229776

RESEARCH ARTICLE

Event-Triggered Auto-Berthing Finite-Time Control for Underactuated Surface Vessel

YANG LIU AND NAM-KYUN IM
Department of Navigation Science, Mokpo National Maritime University, Mokpo 58628, South Korea
Corresponding author: Nam-Kyun Im (namkyun.im@mmu.ac.kr)

This work was supported by the National Research Foundation of Korea (NRF) grant funded by the Korea Government (NRF-2020R1F1A1050113) titled with "The Technology for Marine Traffic Hazard Control system using Ship navigation Big Data".

ABSTRACT An investigation of the auto-berthing problem for underactuated surface vessels is presented, considering dynamic uncertainties, finite time, transmission load, and environmental disturbance constraints. It is proposed to integrate the finite time control technology with the event-triggered mechanism input algorithm to develop a novel control scheme. Applying the differential homeomorphism coordinate method transforms the vessel into a standard integral cascade form to solve the underactuated problem. A finite-time technology and an event-triggered technology are then used to save time for the berthing vessel, decrease the transmission burden between the controller and vessel, and reduce the acting frequency of the actuator. Furthermore, the radial basis function network(RBF) is employed to approximate unknown nonlinear functions, and minimum learning parameters(MLP) are introduced to reduce computational complexity. Based on the Lyapunov stability theory, a sufficient effort has been made to verify the stability of the closed-loop system. The simulation results demonstrate the effectiveness of the proposed scheme.

INDEX TERMS Auto-berthing control, finite-time, underactuated, event-triggered, RBF, MLP.

I. INTRODUCTION

The automatic berthing process refers to the operation of a ship approaching the harbor at an appropriate speed and angle as soon as it enters the port. Therefore, the vessel can stabilize near the berth. It should be noted that the vessel sails at a low speed during berthing. Most vessels are only equipped with two independent stern thrusters or one main stern thruster and rudder, without any thruster installed, further reducing the vessel's maneuverability. Due to this, the auto-berthing control of underactuated vessels have become a relatively complex and challenging task. For the purpose of satisfying the nautical practice and realizing automatic berthing of ships, extensive research has been conducted [1], [2], [3], [4], [5], [6], [7]. Artificial intelligence methods have been used to achieve automatic berthing in [1], [2], [3], and [4]. As a result of engineering considerations such as anti-jamming and multi-port applicability, [1] and [2] realized automatic berthing. Training data are essential in these studies, and it is impossible to control the time ships approach during berthing. Unless the training data are correctly selected, or the quantity is sufficient, automatic berthing cannot be achieved. In [5], [6], and [7], the automatic berthing is implemented utilizing the backstepping method framework in conjunction with the Lyapunov stability principle. In [5] and [6], dynamic surface control is combined to address the problem of the differential explosion that may arise in the control scheme design. As an additional benefit, in [5], the neural network's computational load was reduced using a minimum learning parameter(MLP). A safety-oriented control scheme was developed by [7]. In the designing process, it is necessary to introduce the obstacle Lyapunov function to limit the turning angular velocity of the ship during berthing within a specific range to achieve safe berthing However, this methods also prolongs the time to approach the pier for ships. Nevertheless, the above research does not address the issue of auto-berthing finite time control, and communication resources may be limited, impacting control performance.

Due to the limitations of the port water conditions, ships must ride the tide to enter and leave the port. Whether the tide

The associate editor coordinating the review of this manuscript and approving it for publication was Ton Duc Do.

ride time can be utilized reasonably will impact the operation efficiency and the utilization rate of resources in the harbor. Similarly, when avoiding obstacles in an emergency are necessary, the avoidance cannot be completed within a limited period. As a result of obstruction movements, the port's productivity will also be affected. The solution to this problem is, therefore, reasonable. The hyperbolic tangent guidance method was employed by [8] to control the vessel's course cooperatively, and the controller was designed using terminal non-singular synovial technology. Lastly, the ship is capable of completing the tracking control within a limited period of time. Based on [9], a finite-time disturbance observer estimates the composite disturbance composed of external disturbances and uncertain terms. The virtual control is also derived using finite-time command filtering. Combined with the obstacle Lyapunov function, a trajectory tracking control scheme is developed under total state constraints. According to [10], the non-singular fast terminal sliding mode strategy improves the speed of convergence and the ability of the dynamic positioning system to minimize interference. As a result of [11], synthetic uncertainty parameters and unknown external perturbations were transformed into a linear parameterized form with a single parameter, and finite-time trajectory tracking was solved. Overall, the successful applications of finite-time control in trajectory tracking provide valuable ideas for automatic berthing control in the future.

Autonomous navigation is inextricably linked to the information exchange between the ship and the shore (controller). Much communication will inevitably result in channel congestion and adversely affect the controller's ability to control the ship. As disturbances in ship-to-shore signal transmission may occur in heavy communication workloads, and most navigation control systems use digital processors, it is more appropriate to consider this constraint since it reduces the communication load. By reducing the wear of the actuator, the system can be improved. In [12], a set of control schemes is developed to address this problem using fixed threshold triggering.

On the other hand, [13] has developed a set of event-triggering schemes with a relative threshold strategy, which can relax monitoring restrictions on event triggering. Based on an event-triggered concept, [14] developed a trajectory-tracking control system for surface ships that reduced the computational complexity through MLP. A fault-tolerant trajectory tracking control has been developed by [15], which can ensure stable tracking under the condition that the actuator's action frequency is reduced.

It is imperative to do simulations, or experiments closer to reality [16], [17], [18], [19]. This work focuses on an event-triggered auto-berthing finite-time control approach for underactuated surface vessels and considers the model dynamic uncertainties and external disturbances. To solve the underactuated problem caused by the ship maneuvering model. The vessel is transformed into a standard integral cascade form using differential homeomorphism. Furthermore, system state error variables are established based on the transformation. Combining the finite-time technique, radial basis function network(RBF), MLP, and applying an event trigger mechanism, an event-triggered auto-berthing finite-time control scheme is derived. The stability of a closed-loop control system is demonstrated. The main contributions of this paper are as follows:

(1) By incorporating the finite-time technique in the control design, a viable control method is provided for the auto-berthing control of underactuated marine surface vessels. Compared with [5], [6], and [7], the convergence time of the system manipulation state is significantly reduced. Therefore, the control scheme enables practical implementation.

(2) Compared with auto-berthing control schemes [5], [6], and [7], a relative threshold event-triggered auto-berthing control scheme for underactuated marine surface vessels is developed for the first time. As the communication load is reduced, the wear on the actuator is also reduced, making it more practical to implement.

Following is a summary of the remainder of this article. The second part of the report describes the research questions and preliminary results. The third section provides a detailed discussion of differential homeomorphic coordinate changes. In the fourth part, the controller is designed, and its stability is analyzed. In the fifth section, simulation experiments are presented.

II. PROBLEM FORMULATION AND PRELIMINARIES

A. PROBLEM FORMULATION

According to [20] and [21], vessel model is described as (1) which composed of kinematics and kinetic equations, as shown in FIGURE 1.

$$\begin{cases} \dot{\mathrm{x}} = \mathrm{u}\cos(\psi) - v\sin(\psi) \\ \dot{y} = \mathrm{u}\sin(\psi) - v\cos(\psi) \\ \dot{\psi} = r \\ \dot{u} = \dfrac{m_{22}}{m_{11}}vr - \dfrac{d_u}{m_{11}} - \sum_{i=2}^{3}\dfrac{d_{ui}}{m_{11}}|u|^{i-1}u + \dfrac{\tau_u}{m_{11}} + \dfrac{\tau_{du}}{m_{11}} \\ \dot{v} = -\dfrac{m_{11}}{m_{22}}vr - \dfrac{d_v}{m_{22}} - \sum_{i=2}^{3}\dfrac{d_{vi}}{m_{22}}|v|^{i-1}v + \dfrac{\tau_{dv}}{m_{22}} \\ \dot{r} = \dfrac{m_{11}-m_{22}}{m_{11}}uv - \dfrac{d_r}{m_{33}} - \sum_{i=2}^{3}\dfrac{d_{ri}}{m_{33}}|r|^{i-1}r + \dfrac{\tau_r}{m_{11}} \\ \qquad + \dfrac{\tau_{dr}}{m_{11}} \end{cases} \tag{1}$$

where (x, y) represents the vessel's position, ψ represents the vessel's heading angel. u, v, and r denotes the surge speed, sway speed, and yaw rates. τ_u and τ_r denotes the control input. d_u, d_v, d_r, d_{ui}, d_{vi}, and d_{ri} are hydrodynamic damping. τ_{du}, τ_{dv}, and τ_{dr} are environment disturbance.

B. PRELIMINARIES

Definition 1 [22] : Nonlinear system $\dot{x} = h(x), h(0) = 0, x \in R^n$, where x is the state variable, χ_o is a sphere containing the origin. $h(x)$ is a continuous function, for any initial condition x_0, if there is a constant $c > 0$ and an adjustment time function

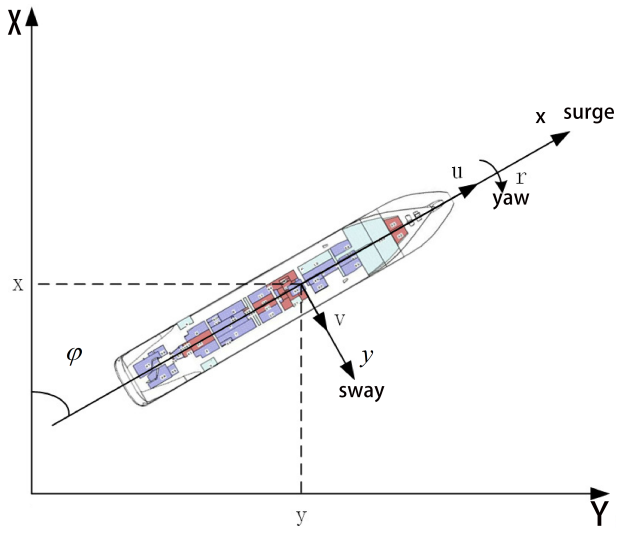

FIGURE 1. Simplified vessel maneuvering coordinate system.

$0 < T(x_0) < \infty$, make $\|x(t)\| \le c$, time variable $t \ge T(x_o)$, T is the time under initial conditions. Then, $h(x)$can be said to be stable in finite time.

Assumption 1: parameters $d_{xi}(x = u, v, r)$ are uncertain.

Assumption 2: disturbances $\tau_{di}(i = u, v, r)$ are bounded, and satisfy $\tau_{di} \le \bar{\tau}_d$.

Lemma 1 [11]: For $x = h(x)$, $h(0) = 0$, $x \in R^n$, where $h(x)$ is a continuous function, suppose there is a continuous Lyapunov function $V : D \to R$ that the following conditions can be established: V is a positive definite function, there exist $\kappa_1 > 0, \kappa_2 > 0, 0 < \alpha < 1$, and an open loop field near the origin satisfies $\dot{V}(x)+\kappa_1 V(x)+\kappa_2 V^{\alpha}(x) \le 0$, then the system is stable in finite time, and the stable time is bounded by

$$T \le \frac{1}{\kappa_1(1-\alpha)} \ln \frac{\kappa_1 V^{(1-\alpha)}(x_0) + \kappa_2}{\kappa_2}. \tag{2}$$

Lemma 2 [7] and [23]: For any unknown nonlinear function $f(x)$, the following RBF network can be used for approximation:

$$f(x) = Wh + \varepsilon \tag{3}$$

where x is the input of RBF; W is an ideal matrix representing the neural networks' weights. $h = h_j(j = 1, 2 \cdots n)$ is the output of the hidden layer, h_j is the activation function that can be described as $h_j = \exp\left(\frac{-\left\|x-c_j^T\right\|^2}{b_j^2}\right)$, c_j is the center vector of the activation function, b_j is is the width of the activation function. ε is the approximation error for RBF network.

Lemma 3 [24] and [25]: For any constant $a > 0$ and any scalar $\varrho \in R$ the following inequality holds:

$$0 \le |\varrho| - \frac{\varrho^2}{\sqrt{\varrho^2 + a^2}} < a \tag{4}$$

III. COORDINATE TRANSFORMATION

Inspired by the literature [26], this paper adopts the differential homeomorphic transformation to solve the underactuated problem of the system (1).

$$h = J^{\mathrm{T}}(\psi)\eta \tag{5}$$

where $h = [h_1, h_2, h_3]^{\mathrm{T}}$, $\eta = [x, y, \psi]^{\mathrm{T}}$, $J(\psi) = \begin{bmatrix} \cos(\psi) & -\sin(\psi) & 0 \\ \sin(\psi) & \cos(\psi) & 0 \\ 0 & 0 & 1 \end{bmatrix}$

Taking the time derivative of (5) yields

$$\dot{h}_1 = \dot{J}^{\mathrm{T}}(\psi)\eta + J^{\mathrm{T}}(\psi)\dot{\eta} \tag{6}$$

$J(\psi)$ satisfies the following properties:

$$\dot{J}^{\mathrm{T}}(\psi) = J(\psi)S(r) \tag{7}$$

where $S(r) = \begin{bmatrix} 0 & -r & 0 \\ r & 0 & 0 \\ 0 & 0 & 0 \end{bmatrix}$.

Then (1) can be written as:

$$\begin{cases} \dot{h}_1 = u + h_2 r \\ \dot{h}_2 = v - h_1 r \\ \dot{h}_3 = r \\ \dot{u} = \frac{m_{22}}{m_{11}} vr - \frac{d_{11}}{m_{11}} u - \sum_{i=2}^{3} \frac{d_{ui}}{m_{11}} |u|^{i-1} u + \frac{\tau_u}{m_{11}} + \frac{\tau_{du}}{m_{11}} \\ \dot{v} = -\frac{m_{11}}{m_{22}} ur - \frac{d_{22}}{m_{22}} v - \sum_{i=2}^{3} \frac{d_{vi}}{m_{22}} |v|^{i-1} v + \frac{\tau_{dv}}{m_{22}} \\ \dot{r} = \frac{m_{11} - m_{22}}{m_{33}} uv - \frac{d_{33}}{m_{33}} r \\ \qquad - \sum_{i=2}^{3} \frac{d_{ri}}{m_{33}} |r|^{i-1} r + \frac{\tau_r}{m_{11}} + \frac{\tau_{dr}}{m_{11}} \end{cases} \tag{8}$$

Let $\sum_{i=2}^{3} \frac{d_{ui}}{m_{11}} |u|^{i-1} u = \frac{f_u}{m_{11}}$, $\sum_{i=2}^{3} \frac{d_{vi}}{m_{11}} |v|^{i-1} v = \frac{f_v}{m_{11}}$, $\sum_{i=2}^{3} \frac{d_{ri}}{m_{11}} |r|^{i-1} u = \frac{f_r}{m_{11}}$, $\tau_1 = \dot{u}, \tau_3 = \dot{r}$, $\frac{m_{22}}{m_{11}} = \frac{1}{A}$, $\frac{d_{22}}{m_{22}} = B$, (8) can be written as

$$\begin{cases} \dot{h}_1 = u + h_2 r \\ \dot{h}_2 = v - h_1 r \\ \dot{h}_3 = r \\ \dot{u} = \tau_1 \\ \dot{v} = -Aur - Bv - \frac{f_v}{m_{22}} + \frac{\tau_{dv}}{m_{22}} \\ \dot{r} = \tau_3 \end{cases} \tag{9}$$

Further, (8) can be transformed as a chain structure system with general nonlinear characteristics by introducing the following variable substitution and feedback transformation [7], [27]

$$\beta_2 = h_2 + \frac{v}{B} \tag{10}$$

Then, $\dot{\beta}_2$ is give

$$\dot{\beta}_2 = \dot{h}_2 + \frac{\dot{v}}{B} = v - h_1 r + \frac{1}{B}(-Aur - Bv)$$

$$= -\left(h_1 + \frac{1}{B}Au\right) r \tag{11}$$

Let $\omega = -\left(h_1 + \frac{1}{B}Au\right)$, one can get

$$\begin{cases} \dot{h}_1 = -\dfrac{B}{A}(\omega + h_1) + \beta_2 r - \dfrac{v}{B}r \\ \dot{\beta}_2 = \omega r - \dfrac{f_v}{d_{22}} + \dfrac{\tau_{dv}}{d_{22}} \\ \dot{h}_3 = r \\ \dot{v} = B(\omega + h_1) r - Bv - \dfrac{f_v}{m_{22}} + \dfrac{\tau_{dv}}{m_{22}} \\ \dot{\omega} = \tau_\omega \\ \dot{r} = \tau_3 \end{cases} \tag{12}$$

Let $\phi_1 = h_1, \phi_2 = \beta_2, \phi_3 = h_3, \phi_4 = v, \phi_5 = \omega, \phi_6 = r, u_1 = \tau_\omega, u_2 = \dot{r} = \tau_3$, the (12) can be written as

$$\begin{cases} \dot{\phi}_1 = -\dfrac{B}{A}(\phi_1 + \phi_5) + \phi_2\phi_6 - \dfrac{1}{B}\phi_4\phi_6 \\ \dot{\phi}_2 = \phi_5\phi_6 + \dfrac{1}{d_{22}}(\tau_{dv} - f_v) \\ \dot{\phi}_3 = \phi_6 \\ \dot{\phi}_4 = B(\phi_1 + \phi_5)\phi_6 - B\phi_4 + \dfrac{1}{m_{22}}(\tau_{dv} - f_v) \\ \dot{\phi}_5 = u_1 \\ \dot{\phi}_6 = u_2 \end{cases} \tag{13}$$

Theorem 1 [28]: For (13), when $t \to \infty$, if $\phi_i (i = 2, 5, 6)$ converges to zero, then, $\lim_{t\to\infty} \phi_i = 0 (i = 1, 4)$

$$\begin{cases} \dot{\phi}_2 = \phi_5 Z_6 \\ \dot{\phi}_3 = \phi_6 \\ \dot{\phi}_5 = u_1 \\ \dot{\phi}_6 = u_2 \end{cases} \tag{14}$$

Let $x_1 = \phi_3, x_2 = \phi_6, x_3 = \phi_2, x_4 = \phi_5$ yields

$$\begin{cases} \dot{x}_1 = x_2 \\ \dot{x}_2 = u_2 \\ \dot{x}_3 = x_4 x_2 + \dfrac{1}{d_{22}}(\tau_{dv} - f_v) \\ \dot{x}_4 = u_1 \end{cases} \tag{15}$$

IV. CONTROLLER DESIGN AND STABILITY ANALYSIS

A. CONTROLLER DESIGN

In this article, the control system for underactuated marine surface vessels is devised in FIGURE 2. Only at triggering instants control signals of the finite-time controller will be sent to the ship. Based on this frame, the following part of this section proposes an adaptive neural network automatic berthing control considering finite time and an event-triggered mechanism. It ensures the final bounded consistency of all signals in the closed-loop control system of an underactuated vessel, which is affected by dynamic uncertainties and external disturbances. By selecting the system error and constructing an appropriate Lyapunov function, a finite-time automatic berthing control law that can

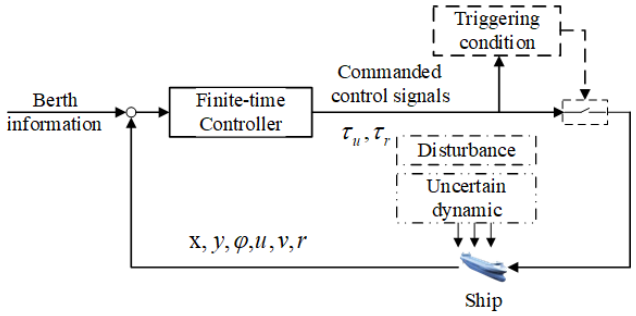

FIGURE 2. Frame of the control system.

reduce the communication load is designed for the system. According to (15), define the following error variable

$$z_1 = x_1 - x_{1d} \tag{16}$$

$$z_2 = x_2 - \rho_1 \tag{17}$$

where $z_i (i = 1, 2)$ is the defined systematic error. x_{1d} represents the expected state x_1, which is a constant. ρ_1 is a intermediate control variable.

Take the derivative of z_1, and using (17) yields

$$\dot{z}_1 = z_2 + \rho_1 \tag{18}$$

Design the Intermediate control variable ρ_1 as

$$\rho_1 = -k_1 z_1 - k_{11}\frac{z_1}{\sqrt{z_1^2 + \delta_1^2}} \tag{19}$$

where k_1, k_{11} is a positive parameter waiting to be set, $\delta_1 > 0$ is a constant.

To stabilize the error variable z_1 and z_2, We choose the intermediate control adaptive state variable $\hat{\theta}_r$ as in (20) and control input τ_r, where $g = \frac{m_{11}-m_{22}}{m_{33}}uv - \frac{d_{33}}{m_{33}}r$, $k_1, k_{11}, k_{22}, \delta_2$, and σ_r positive parameters, $\zeta_r(v)$ is the scalar associated with the hidden layer in the RBF network, which have specific expressions in the stability analysis of the system.

$$\begin{cases} \tau_r(\mathrm{t}) = \hat{\tau}_r(t_k); \forall t \in [t_k, t_{k+1}] \\ \hat{\tau}_r(t_k) = m_{33}\left(-g - k_1 x_2 - k_{11}\dfrac{x_2}{\sqrt{z_1^2 + \delta^2}} - z_1\right. \\ \left. -k_{22}\dfrac{z_2}{\sqrt{z_2^2 + \delta_2^2}} - c_1 z_2 \hat{\theta}_r \zeta_r^2(v) - k_2 z_2\right) \\ \dot{\hat{\theta}}_r = c_1 z_2^2 \zeta_r^2(v) - \sigma_r \hat{\theta}_r \\ t_{k+1} = \inf\{t \in R; |e| \geq \Gamma_r |\tau_r(t)| + D_r\} \\ e_r = \hat{\tau}_r - \tau_r; \end{cases} \tag{20}$$

Define the following error variable

$$z_3 = x_3 - x_{3d} \tag{21}$$

$$z_4 = x_4 - \rho_2 \tag{22}$$

where $z_i (i = 3, 4)$ is the defined systematic error. x_{3d} represent the desired state x_3, which is a constant. ρ_2 is a intermediate control variable.

Take the derivative of z_3, and using (23)

$$\dot{z}_3 = (z_3 + \rho_2)\, x_2 + \frac{1}{d_{22}}\left(\tau_{dv} - f_v\right) \tag{23}$$

Design the intermediate control variable ρ_2 as

$$\rho_2 = -k_3 z_3 x_2 - k_{12}\frac{z_3 x_3}{\sqrt{z_3^2 + \delta_3^2}} \tag{24}$$

where k_3 and k_{12} are positive parameters.

To stabilize the error variable z_3 and z_4, we choose the adaptive state variable $\hat{\theta}_u$ as (25) and control input τ_{u}, where $f = \left(\frac{d_{11}}{d_{22}} - 1\right)u - \dot{\rho}_2$, k_4, k_{33}, and σ_u are positive parameters, $\zeta_u(v)$ is a scalar related to the hidden layer in the RBF network, and will be stated explicitly in the stability analysis of the system.

$$\begin{cases} \tau_u(t) = \hat{\tau}_u(t_k);\, \forall t \in [t_k, t_{k+1}]) \\ \hat{\tau}_u(t_k) = d_{22}\left(f + k_4 x_4 - k_{33}\dfrac{z_4}{\sqrt{z_4^2 + \delta_4^2}} + c_3 z_4 \hat{\theta}_u \zeta_u^2(v)\right) \\ \dot{\hat{\theta}}_u = c_3 z_4^2 \zeta_r^2(v) - \sigma_u \hat{\theta}_u \\ t_{k+1} = \inf\{t \in R;\, |e| \geq \Gamma_u |\tau_u(t)| + D_u\} \\ e_u = \hat{\tau}_u - \tau_u \end{cases} \tag{25}$$

Synthesizing (20) and (25), one can obtain

$$\begin{cases} \hat{\tau}_u = d_{22}\left(f + k_4 x_4 - k_{33}\dfrac{z_4}{\sqrt{z_4^2 + \delta^2}} + c_3 z_4 \hat{\theta}_u \zeta_u^2(v)\right) \\ \hat{\tau}_r = m_{33}\left(-g - k_1 x_2 - k_{11}\dfrac{x_2}{\sqrt{z_1^2 + \delta^2}} - z_1\right. \\ \left. -k_{22}\dfrac{z_2}{\sqrt{z_2^2 + \delta^2}} - c_1 z_2 \hat{\theta}_r \zeta_r^2(v) - k_2 z_2\right) \end{cases} \tag{26}$$

with adaptive control scheme

$$\begin{cases} \dot{\hat{\theta}}_r = c_1 z_2^2 \zeta_r^2(v) - \sigma_r \hat{\theta}_r \\ \dot{\hat{\theta}}_u = c_3 z_4^2 \zeta_r^2(v) - \sigma_u \hat{\theta}_u \end{cases} \tag{27}$$

and event-triggered mechanism

$$\begin{cases} \tau_i(t) = \hat{\tau}_i\left(t_k\right);\, \forall t \in [t_k, t_{k+1}] \\ t_{k+1} = \inf\{t \in R;\, |e| \geq \Gamma_i |\tau(t)| + D_i\} \\ e_i = \hat{\tau}_i - \tau_i \\ i = (u, r) \end{cases} \tag{28}$$

where $0 < \Gamma_i < 1$, D_i is a positive parameter that will trigger the rules and the performance of the automatic berthing control for underactuated vessels. Constructing a new Lyapunov function for stability analysis of closed-loop systems:

$$V = \frac{1}{2}z_1^2 + \frac{1}{2}z_2^2 + \frac{1}{2}z_3^2 + \frac{1}{2}z_4^2 + \frac{1}{2}\tilde{\theta}_u^2 + \frac{1}{2}\tilde{\theta}_v^2 + \frac{1}{2}\tilde{\theta}_r^2 \tag{29}$$

Taking the derivative of V, and using (18) and (24) one can get

$$\begin{aligned} \dot{V} &= z_1 z_2 - k_1 z_1^2 - k_{11}\frac{z_1^2}{\sqrt{z_1^2 + \delta_1^2}} + z_2\left(g + \frac{\tau_r}{m_{33}} - \frac{f_r}{m_{33}}\right. \\ &\left. + \frac{\tau_{dr}}{m_{33}} + k_1 x_2 + k_{11}\frac{x_2}{\sqrt{z_1^2 + \delta_1^2}}\right) - k_3 z_3^2 x_2^2 - k_{12}\frac{z_3^2 x_2^2}{\sqrt{z_3^2 + \delta_3^2}} \\ &+ z_3\left(\frac{\tau_{dv} - f_v}{d_{22}}\right) + z_4\left[f - \frac{\tau_u + f_u - \tau_{du}}{d_{22}}\right] - \frac{1}{2}\tilde{\theta}_{\mathrm{u}}\dot{\tilde{\theta}}_u \\ &- \frac{1}{2}\tilde{\theta}_v\dot{\tilde{\theta}} - \frac{1}{2}\tilde{\theta}_r\dot{\tilde{\theta}}_r \end{aligned} \tag{30}$$

According to lemma 2, using RBF to approximate $-\frac{f_r}{m_{33}}$, $-\frac{f_v}{d_{22}}$ and $\frac{f_u}{d_{22}}$, and combined with MLP technology, the external disturbance. Then, we can write the external disturbance and uncertain dynamics as

$$\left\| w_i^* s_i(v) + \varepsilon_i + \frac{\tau_{wi}}{m_{33}} \right\| \leq \theta_i \zeta_i(v) (i = v, r) \tag{31}$$

$$\left\| w_u^* s_u(v) + \varepsilon_u - \frac{\tau_{wu}}{m_{33}} \right\| \leq \theta_u \zeta_u(v) \tag{32}$$

where $\theta_i = \max\left\{w_i^*, \varepsilon_i + \frac{\tau_{wi}}{m_{33}}\right\}(i = v, r)$, $\zeta_i(v) = \|S_i(v)\| + 1(i = v, r)$, $\theta_u = \max\left\{w_u^*, \varepsilon_u - \frac{\tau_{wu}}{m_{33}}\right\}$ $\zeta_u(v) = \|S_u(v)\| + 1$.

Combine (26), (27), (28), (30), (32), and apply the following Young's inequality [7]: $z_2\theta_r\zeta_r(v) \leq c_1\theta_r\zeta_r^2(v)z_2^2 + \frac{\theta_r}{4c_1}$, $z_3\theta_v\zeta_v(v) \leq c_2\theta_v\zeta_v^2(v)z_3^2 + \frac{\theta_v}{4c_2}$, $z_4\theta_u\zeta_u(v) \leq c_3\theta_u\zeta_u^2(v)z_4^2 + \frac{\theta_u}{4c_3}$, $\tilde{\theta}_u\hat{\theta}_u \leq -\frac{1}{2}\tilde{\theta}_u^2 + \frac{1}{2}\theta_u^2$, $\tilde{\theta}_v\hat{\theta}_v \leq -\frac{1}{2}\tilde{\theta}_v^2 + \frac{1}{2}\theta_v^2$, and $\tilde{\theta}_r\hat{\theta}_r \leq -\frac{1}{2}\tilde{\theta}_r^2 + \frac{1}{2}\theta_r^2$, where c_1, c_2, and c_3 are the parameters to be designed. Then, (30) can be written as

$$\begin{aligned} \dot{V} \leq\ & -k_1 z_1^2 - k_{11}\frac{z_1^2}{\sqrt{z_1^2 + \delta_1^2}} - k_2 z_2^2 - k_{22} \\ & -k_4 z_4^2\frac{z_2^2}{\sqrt{z_2^2 + \delta_2^2}} - k_3 z_3^2 x_2^2 - k_{12}\frac{z_3^2 x_2^2}{\sqrt{z_3^2 + \delta_3^2}} \\ & -\frac{k_{33} z_4^2}{\sqrt{z_4^2 + \delta_4^2}} - \frac{1}{2}\tilde{\theta}_{\mathrm{u}}^2 - \frac{1}{2}\tilde{\theta}_r^2 - \frac{1}{2}\tilde{\theta}_v^2 + \mathrm{c}_2\theta_v\zeta_v^2(v)z_3^2 \\ & + \frac{\theta_u}{4c_3} + \frac{\theta_v}{4c_2} + \frac{\theta_r}{4c_1} + \frac{1}{2}\theta_{\mathrm{u}}^2 + \frac{1}{2}\theta_r^2 + \frac{1}{2}\theta_v^2 \end{aligned} \tag{33}$$

On the right side of (33) adding and subtracting $\frac{1}{z}\left|\tilde{\theta}_u\right|, \frac{1}{z}\left|\tilde{\theta}_r\right|, \frac{1}{z}\left|\tilde{\theta}_v\right|$ and using Young's inequality [11] yields, $\frac{l_i}{z}\left|\tilde{\theta}_i\right| \leq \frac{l_i}{4}\left|\tilde{\theta}_i\right|^2 + \frac{l_i}{4}(i = u, v, r)$, where l_i is a positive parameter. According to lemma 3, we can get $-\frac{z_1^2}{\sqrt{z_1^2+\delta_1^2}} \leq \delta_1 - |z_1|$, $-\frac{z_2^2}{\sqrt{z_2^2+\delta_2^2}} \leq \delta_2 - |z_2|$, $-\frac{z_3^2}{\sqrt{z_3^2+\delta_3^2}} \leq \delta_3 - |z_3|$,

$-\frac{z_4^2}{\sqrt{z_4^2+\delta_4^2}} \leq \delta_4 - |z_4|$, then (33) can be written as

$$\begin{aligned}\dot{V} \leq & -k_1 z_1^2 - k_2 z_2^2 - k_3 z_3^2 x_2^2 - k_4 z_4^2 \\ & -\left(\frac{1}{2}-\frac{l_u}{4}\right)\tilde{\theta}_{\mathrm{u}}^2 - \left(\frac{1}{2}-\frac{l_r}{4}\right)\tilde{\theta}_r^2 - \left(\frac{1}{2}-\frac{l_v}{4}\right)\tilde{\theta}_v^2 \\ & -k_{11}|z_1| - k_{22}|z_2| - k_{12}x_2^2|z_3| - k_{33}|z_4| \\ & -\frac{1}{2}\left|\tilde{\theta}_u\right| - \frac{1}{2}\left|\tilde{\theta}_v\right| - \frac{1}{2}\left|\tilde{\theta}_r\right| + \mathrm{c}_2\theta_v\zeta_v^2(v)z_3^2 \\ & +\frac{\theta_u}{4c_3} + \frac{\theta_v}{4c_2} + \frac{\theta_r}{4c_1} + \frac{1}{2}\theta_{\mathrm{u}}^2 + \frac{1}{2}\theta_r^2 + \frac{1}{2}\theta_v^2 \\ & +k_{11}\delta_1 + k_{22}\delta_2 + k_{12}x_2^2\delta_3 + k_{33}\delta_4 + \frac{l_u+l_v+l_r}{4} \\ \leq & -\vartheta_1 V - \vartheta_2 V^{\frac{1}{2}} + \vartheta \end{aligned} \tag{34}$$

where $\vartheta_1 = \min\left\{k_1, k_2, k_3x_2^2, k_4, \left(\frac{1}{2}-\frac{l_u}{4}\right), \left(\frac{1}{2}-\frac{l_r}{4}\right)\left(\frac{1}{2}-\frac{l_v}{4}\right)\right\}$, $\vartheta_2 = \min\left\{k_{11}, k_{22}, k_{12}x_2^2, k_{33}, \frac{1}{2}\right\}$, $\vartheta = \left(\mathrm{c}_2\theta_v\zeta_v^2(v)z_3^2 + \sum\frac{\theta_i}{4c_j} + \sum\frac{1}{2}\theta_i^2 + k_{11}\delta_1 + k_{22}\delta_2 + k_{12}x_2^2\delta_3 + k_{33}\delta_4 + \sum\frac{l_i}{4}\right)(i = u, v, r\ j = 1, 2, 3;)$

B. STABILITY ANALYSIS

For the underactuated model (1), by designing a control scheme (26), an adaptive control scheme (27), and an event-triggered mechanism (28), which can make the vessel automatically sail (x, y, ψ) to (x_d, y_d, ψ_d), and the error variable z_1, z_2, z_3, and z_4 gather in a minimal range within a limited time, which shows that in a closed-loop system all signals are bounded. Through (34) we can get $\dot{V} \leq -\vartheta_1 V + \vartheta$ that shows the designed Lyapunov function V is uniformly bounded, $z_i(i = 1, 2, 3, 4)$ and $\tilde{\theta}_j(j = u, v, r)$ are all bounded. Since x_{1d} and x_{3d} are constant and combine (16) and (21), we can see that x_1, x_3, and ρ_1 are all bounded, then x_2 bounded, On this basis, combine Equation (24) we can see that ρ_2 is bounded. To sum up, it can be concluded that τ_u and τ_r composed of the above variables are also bounded. Therefore, all signals in a closed-loop system are bounded. Recalling (34), one can get

$$\dot{V} \leq -\mu\vartheta_1 V - (1-\mu)\vartheta_1 V - \vartheta_2 V^{\frac{1}{2}} + \vartheta \tag{35}$$

where $0 < \mu < 1$, if $V > \frac{\vartheta}{\mu\vartheta_1}V$, we have

$$\dot{V} \leq -(1-\mu)\vartheta_1 V - \vartheta_2 V^{\frac{1}{2}} \tag{36}$$

According to lemma 1, V settles within the residual set $\varpi = \left\{V \leq \frac{\vartheta}{\mu\vartheta_1}\right\}$, and the settling time is

$$T \leq \frac{4}{(1-\mu)\vartheta_1}\ln\left(\frac{(1-\mu)\vartheta_1 V^{\frac{1}{2}}(0) + \vartheta_2}{\vartheta_2}\right) \tag{37}$$

where $V(0)$ is the initial value of V. During the trigger hold phase of the system $[t_k, t_{k+1})$, the control scheme τ_u and τ_r will be kept as a constant value. Take the derivative of $e_i = \hat{\tau}_i - \tau_i(i = u, r)$ one can get

$$\frac{d\,|e_i|}{dt} = \frac{d}{dt}(e_i * e_i) = \mathrm{sign}\,(e_i)\,\dot{e}_i \leq \left|\dot{\hat{\tau}}_i\right| \tag{38}$$

TABLE 1. Model parameters and design parameters.

Indexes	Items	value	Items	value
Model Parameters	m	17.6 kg	m_{33}	80 kg
	L	1.19 m	d_{11}	70 kg/s
	m_{11}	200 kg	d_{22}	100 kg/s
	m_{22}	250 kg	d_{33}	50 kg · m^2/s
Design Parameters	k_1	0.5	c_1	0.00014
	k_2	0.12	c_2	0.001
	k_3	2	σ_r	0.00001
	k_4	4.1	σ_u	0.00002
	δ_1	150	Γ_u	0.4
	δ_2	150	Γ_r	0.3
	δ_3	150	D_u	0.3
	δ_4	150	D_r	0.013

where $\hat{\tau}_i$ is a function that composed of $z_i, x_i(i = 1, 2, 3, 4)$, $\rho_1, \rho_2, \hat{\theta}_u, \hat{\theta}_r$. From the previous analysis, it can be seen that $\hat{\tau}_i$ is bounded. Take the derivative of $\hat{\tau}_i$ yields

$$\begin{cases}\dot{\hat{\tau}}_u = \dfrac{\partial\hat{\tau}_u}{\partial f}\dfrac{\partial f}{\partial\dot{\rho}_2}\dfrac{\partial\dot{\rho}_2}{\partial z_3}\dot{z}_3 + \dfrac{\partial\hat{\tau}_u}{\partial x_4}\dot{x}_4 + \dfrac{\partial\hat{\tau}_u}{\partial z_4}\dot{z}_4 + \dfrac{\partial\hat{\tau}_u}{\partial\hat{\theta}_u}\dot{\theta}_u \\ \dot{\hat{\tau}}_r = \dfrac{\partial\hat{\tau}_r}{\partial x_2}\dot{x}_2 + \dfrac{\partial\hat{\tau}_r}{\partial z_1}\dot{z}_1 + \dfrac{\partial\hat{\tau}_r}{\partial z_2}\dot{z}_2 + \dfrac{\partial\hat{\tau}_r}{\partial\hat{\theta}_r}\dot{\hat{\theta}}_r\end{cases} \tag{39}$$

From formula (39), it can be known that, $\dot{\hat{\tau}}_i(i = u, r)$ is a smooth differentiable function, $\dot{\hat{\tau}}_i$ is a continuous function. From (16)-(18), (22), (23), (27), it can be seen that $\dot{z}_i(i = 1, 2, 3, 4)$ and $\dot{\hat{\theta}}_i(i = u, v)$ are bounded. So there exists $\bar{\tau} > 0$, and satisfys $|\dot{\hat{\tau}}_i| \leq \bar{\tau}$. Using proof by contradiction, assume that events trigger control scheme (28) exists the Zeno phenomenon, that is to say, when $\Delta t = t_{k+1} - t_k = 0$, $\frac{d|e_i|}{dt} = \lim_{t\to t_{k+1}}\frac{|e_i(t)|-|e_i(|e_i(t)|)|}{t-t_{k+1}}$ does not exist. However, as illustrated in (38), $\Delta t \neq 0$ exists. Therefore the trigger mechanism does not trigger the Zeno phenomenon.

V. SIMULATIONS

In this part, the effectiveness of the proposed control scheme is evaluated using a simulation using CyberShip I. A set of initial parameters is chosen for the ship as $[x(0), y(0), \psi(0), u(0), v(0), r(0)] = [-10\,L, -10\,L, \frac{\pi}{3}, 0.2, 0, 0]$. Berthing goals are designed as $[x_d, y_d, \psi_d] = [0\,L, 0\,L, 0\mathrm{rad}]$. According to assumption 2, the disturbance of $[d_u, d_v, d_r]$ is designed as$[0.001 * cos(0.8 * \pi * t + 0.2, 0.001 * sin(0.8 * \pi * t + 0.4, 0.001 * cos(0.8 * \pi * t + 0.2]$. Model parameters and design parameters can be found at [29], as well as listed in TABLE 1.

A group of comparisons are provided to evaluate the performance of the designed control scheme among plan 1, plan 2, and plan 3.

Plan 1 (FT+ET+RBF+MLP): Control scheme (26) proposed in this paper, in which finite-time control(FT), event-triggered mechanism(ET), RBF, and MLP are adopted.

Plan 2 (ET+RBF+MLP): The continuous control scheme (26), based on plan one but without an event-triggered mechanism(28), only adopts FT, RBF, and MLP. The proof of the stability of the continuous control scheme is omitted. One can refer to the evidence of the proposed control scheme in this paper.

TABLE 2. Stabilization time.

Indexes	Plan 1	Plan 2	Plan 3
x/L	15.06 s	15.04 s	16.2 s
y/L	16.4 s	15.05 s	27.46 s
ψ	15.28 s	14.47 s	17.4 s

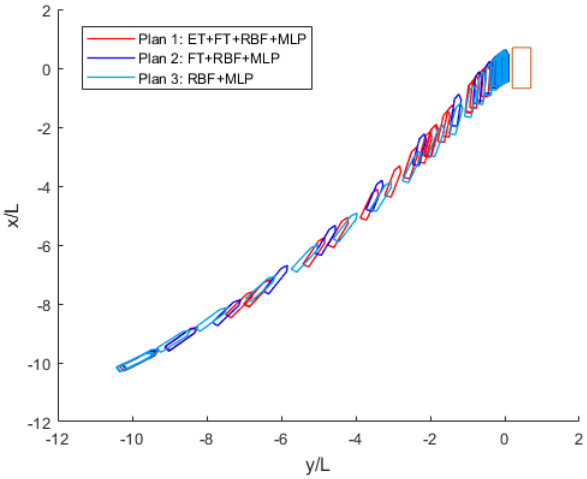

FIGURE 3. Comparison of vessel trajectorys among plan 1, plan 2, and plan 3.

Plan 3 (RBF+MLP): Control scheme (40), which only uses RBF, and MLP technology, as shown in (40).The stability proof process of control scheme (40) is similar to that described in [5] and [7].

$$\begin{cases} \bar{\tau}_u = d_{22}\left[\left(\dfrac{\mathrm{d}_{11}}{d_{22}} - 1\right)u + k_4 e_4 + \mathrm{c}_3\hat{\theta}_u\xi_u^2(\mathrm{v})e_4\right] \\ \bar{\tau}_r = m_{33}\left(-k_2 e_2 - k_1 x_2 - \dfrac{m_{11}-m_{33}}{m_{33}}uv + \dfrac{d_{33}}{m_{33}}r\right. \\ \left. -e_1 - \mathrm{c}_1\hat{\theta}_r\xi_r^2(\mathrm{v})e_2\right. \\ \dot{\hat{\theta}}_{\mathrm{u}} = c_3\xi_u^2(\mathrm{v})e_4^2 - \beta_u\hat{\theta}_{\mathrm{u}} \\ \dot{\hat{\theta}}_r = c_1\xi_r^2(\mathrm{v})e_2^2 - \beta_r\hat{\theta}_r \end{cases} \tag{40}$$

Through the comparisons between plan 1 and plan 2, the effect of the event-triggered mechanism on the system can be known. By comparing plan 1, plan 2, and plan 3, the impact of finite-time technology on the system can be known. The initial state of the contrast object is the same when simulating, so the comparison can be guaranteed to be fair. A summary of the results can be found in FIGURES 3-9 and TABLE 2.

FIGURE 3 illustrates the trajectory under control plan 1 (red), plan 2(dark blue), and plan 3(light blue). As can be seen, all the control schemes make the ship achieve automatic berthing, but the ship under the control of plan 2 is ahead of other vessels, then is the ship under plan 1, and the last one is the ship under plan 3.

In addition, to quantitatively analyze the performance of the underactuated marine surface vessels under finite-time control and without finite-time control, the duration curves of the ship states x, y, and ψ are plotted in FIGURE 4, and the detail stabilization time is listed in TABLE 2. In FIGURE 4, x/L represents the vessel's movement in the vertical direction, y/L represents the movement in the horizontal direction, and ψ represents the change curve of the ship's heading from $\pi/3$ to 0. As can be seen, both the dark blue curve and the red curve convergence to the target position faster than the light blue curve, which verifies the effectiveness of our proposed control schemes as they converge faster. In other words, the ship, with the control of plan 1 and plan 2, can stabilize at the pier faster. Moreover, we found that the dark blue curve converges faster than the red curve because the closed-loop system summarizes the continuous control scheme, which can take advantage of the position information provided by the ship in real-time to achieve a more effective control effect. The above phenomenon has also been validated in the trajectory tracking research of [12] and [14].

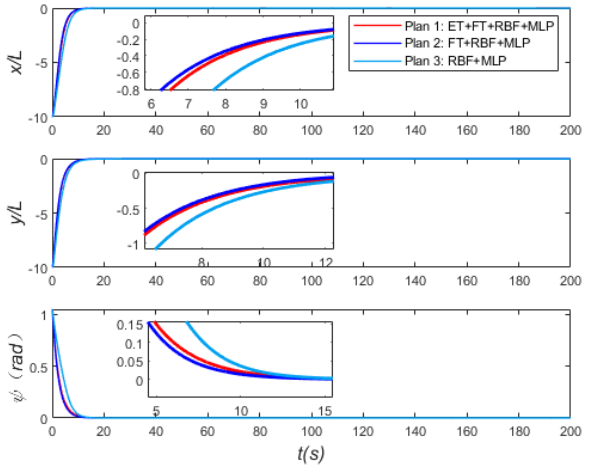

FIGURE 4. Comparison of x,y, and ψ among plan 1, plan 2, and plan 3.

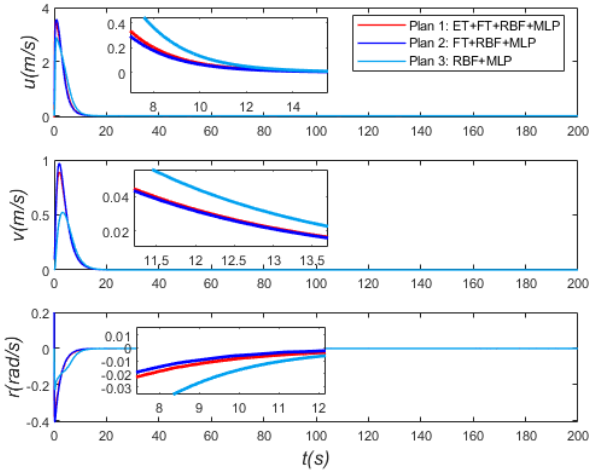

FIGURE 5. Comparison of u,v, and r among plan 1, plan 2, and plan 3.

Remark: x/L and y/L are dimensionless processing of ship maneuvering coordinates so that the influence of units can be avoided.

FIGURE 5 plots u, v, and r versus time, and it can be seen that they are all bounded. Through the analysis of FIGURE 4, it is easy to imagine that the change regulation of the curve in FIGURE 5 should be the same as in FIGURE 4. The value of

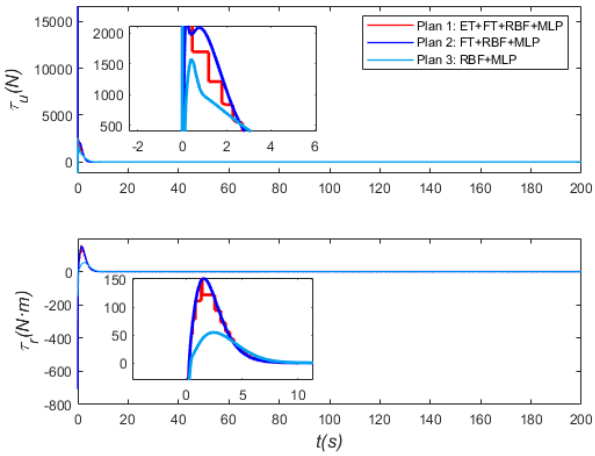

FIGURE 6. Comparison of τ_u and τ_r among plan 1, plan 2, and plan 3.

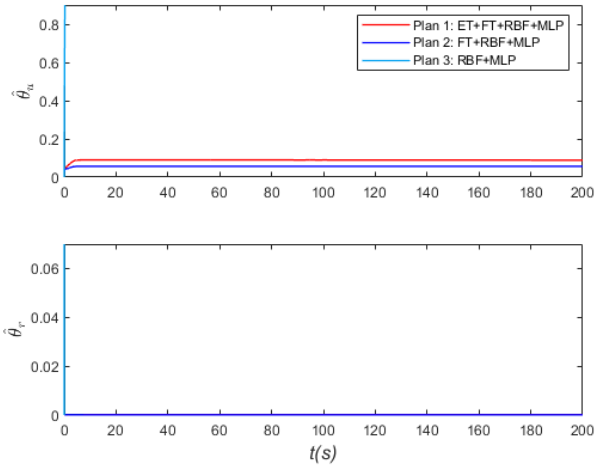

FIGURE 7. Comparison of $\hat{\theta}_u$ and $\hat{\theta}_r$ among plan 1, plan 2, and plan 3.

TABLE 3. Number of events.

	τ_u	τ_r
Plan 1/Plan 2	161/5544	437/5544

the dark blue curve is the largest at a specific moment before reaching the stable position, followed by the red and light blue curves.

FIGURE 6 illustrates the curve change of control input under plan 1, plan 2, and plan 3. The top half of FIGURE 6 and the bottom half of FIGURE 6 represent the control input of surge force τ_u and sway yaw moment τ_r, respectively. The red curve in FIGURE 6 is composed of many straight-line segments, which demonstrates that the event-triggering mechanism we set has played a role. The control input will have a new updated value only when the trigger condition is met; otherwise, it will remain a constant value, which proves that our control scheme is valid.

FIGURE 7 shows the curve of the adaptive parameters, as can be seen that all parameters are bounded. In FIGURES 8 and 9, the abscissa position of the blue line represents the moment when the event occurs, and the length of the blue line represents the time interval between two adjacent trigger events. Statistics reveal that the minimum

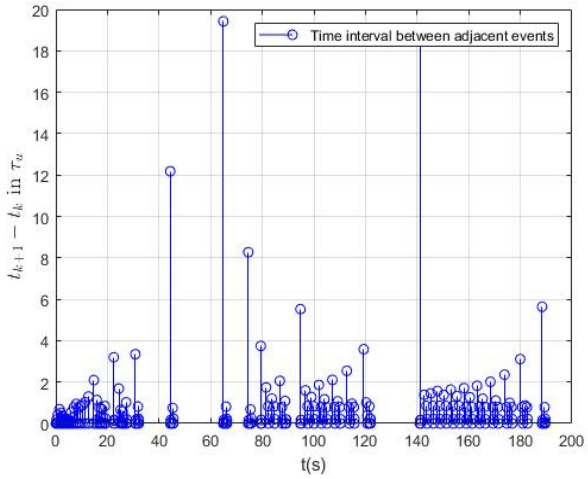

FIGURE 8. Events moment and the time interval between adjacent events of τ_u.

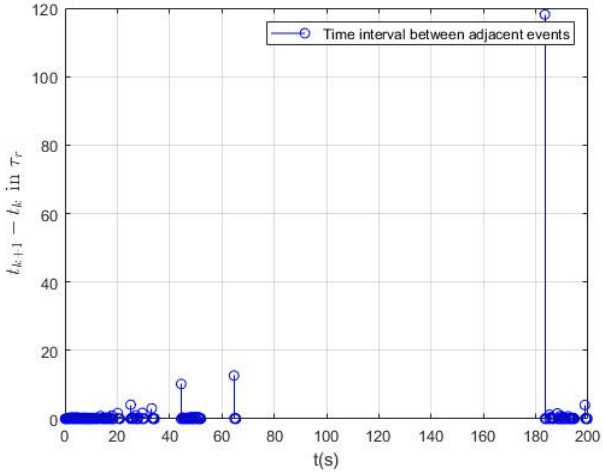

FIGURE 9. Events moment and the time interval between adjacent events of τ_r.

trigger interval of τ_u is $3.3e-16$ seconds, and the maximum is 19.42 seconds; the minimum trigger interval of τ_r is $1e-14$ seconds which happened in the initial stage, and the maximum is 118 seconds. From the above analysis, we can see that the control scheme we designed avoids the Zeno effect. TABLE 3 shows the statistics regarding the events that be triggered. In 200 s, the real events are 161 and 437 in channel τ_u and channel τ_r, respectively. Under the event-triggered control, besides completing the automatic berthing process, the ship also saves a lot of communication load and reduces the wear on the actuators. which in turn, saves 97% of the communication resources and 92% of the communication resources, respectively. Compared to [5], [6], and [7], the communication load decreases significantly.

VI. CONCLUSION

A finite-time auto-berthing control scheme that considers the communication load has been proposed for an underactuated vessel with uncertain model dynamics and external disturbances. To solve the problem of underactuated, we are using a differential homeomorphism transformation approach. Based

on the backstepping framework, we propose an event-triggered auto-berthing finite time control scheme combining finite time control theory, RBF, MLP, and event-triggered mechanisms. RBF provides an efficient means of approximating uncertain dynamics. In addition, MLP is used to increase the calculation's efficiency. Since the convergence time of this method is faster than the auto-berthing control scheme without considering finite time theory, it has been able to realize relatively efficient berthing operations compared with the auto-berthing control scheme without considering finite time theory. In contrast to the auto-berthing control scheme without an event-triggered mechanism, the performance of the berthing controller can be guaranteed by our method. Meanwhile, it reduces the communication load and reduces actuator wear. According to the Lyapunov-based theoretical analysis, all signals within the proposed auto-berthing control scheme are bounded.

In this paper, the event-triggered mechanism has been used to address the issue of communication load in this work. However, the impact of communication delay or transmission error on the control in actual practice is also an essential factor. Further studies will be conducted to investigate solutions for automatic berthing control if an actuator fails.

REFERENCES

[1] H. Yamato, H. Uetsuki, and T. Koyama, "Automatic berthing by neural controller," in *Proc. SCSS*, 1990, pp. 183–201.

[2] N. K. Im and K. Hasegawa, "Motion identification using neural networks and its application to automatic ship berthing under wind," *J. Ship Ocean Technol.*, vol. 6, no. 1, pp. 16–26, Mar. 2002.

[3] N.-K. Im and V.-S. Nguyen, "Artificial neural network controller for automatic ship berthing using head-up coordinate system," *Int. J. Nav. Archit. Ocean Eng.*, vol. 10, no. 3, pp. 235–249, 2018.

[4] S. Hong and J. Kim, "Reinforcement learning based tugboats control for autonomous ship berthing," *J. KNST*, vol. 4, no. 1, pp. 72–77, Mar. 2021.

[5] Z. Qiang, Z. Guibing, H. Xin, and Y. Renming, "Adaptive neural network auto-berthing control of marine ships," *Ocean Eng.*, vol. 177, pp. 40–48, Apr. 2019.

[6] Y. Zhang, M. Y. Zhang, and Q. Zhang, "Auto-berthing control of marine surface vehicle based on concise backstepping," *IEEE Access*, vol. 8, pp. 197059–197067, 2020.

[7] Y. Liu, N.-K. Im, Q. Zhang, and G. Zhu, "Adaptive auto-berthing control of underactuated vessel based on barrier Lyapunov function," *J. Mar. Sci. Eng.*, vol. 10, no. 2, p. 279, Feb. 2022.

[8] N. Wang and C. K. Ahn, "Hyperbolic-tangent LOS guidance-based finite-time path following of underactuated marine vehicles," *IEEE Trans. Ind. Electron.*, vol. 67, no. 10, pp. 8566–8657, Oct. 2019.

[9] Y. M. Hu, S. H. Yu, Y. Yan, and Y. Zhao, "Finite time trajectory tracking control of ocean surface vessels based on command filtering with full state constraints," *J. Nanjing Univ. Sci. Technol.*, vol. 45, no. 3, pp. 271–280, Jun. 2021.

[10] H. L. Chen, H. X. Ren, and B. C. Yang, "Design of finite time controller for ship dynamic positioning based on LS-SVM," *J. Nanjing Univ. Sci. Technol.*, vol. 42, no. 2, pp. 77–84, Feb. 2020.

[11] G. Zhu, Y. Ma, and S. Hu, "Single-parameter-learning-based finite-time tracking control of underactuated MSVs under input saturation," *Control Eng. Pract.*, vol. 105, Dec. 2020, Art. no. 104652.

[12] P. Tabuada, "Event-triggered real-time scheduling of stabilizing control tasks," *IEEE Trans. Autom. Control*, vol. 52, no. 9, pp. 1680–1685, Sep. 2007.

[13] A. Girard, "Dynamic triggering mechanisms for event-triggered control," *IEEE Trans. Autom. Control*, vol. 60, no. 7, pp. 1992–1997, Jul. 2015.

[14] Y. Deng, X. Zhang, N. Im, G. Zhang, and Q. Zhang, "Model-based event-triggered tracking control of underactuated surface vessels with minimum learning parameters," *IEEE Trans. Neural Netw. Learn. Syst.*, vol. 31, no. 10, pp. 4001–4014, Oct. 2020.

[15] G. Zhu, Y. Ma, Z. Li, R. Malekian, and M. Sotelo, "Event-triggered adaptive neural fault-tolerant control of underactuated MSVs with input saturation," *IEEE Trans. Intell. Transp. Syst.*, vol. 23, no. 7, pp. 7045–7057, Jul. 2022.

[16] X. Xiao, B. M. Roh, and F. Zhu, "Strength enhancement in fused filament fabrication via the isotropy toolpath," *Appl. Sci.*, vol. 11, no. 13, p. 61000, Sep. 2021.

[17] X. Xiao, S. Joshi, and J. Cecil, "Critical assessment of shape retrieval tools (SRTs)," *Int. J. Adv. Manuf. Technol.*, vol. 116, nos. 11–12, pp. 3431–3446, Oct. 2021.

[18] X. Xiao, C. Waddell, C. Hamilton, and H. Xiao, "Quality prediction and control in wire arc additive manufacturing via novel machine learning framework," *Micromachines*, vol. 13, no. 1, p. 137, Jan. 2022.

[19] X. Xiao, B.-M. Roh, and C. Hamilton, "Porosity management and control in powder bed fusion process through process-quality interactions," *CIRP J. Manuf. Sci. Technol.*, vol. 38, pp. 120–128, Aug. 2022.

[20] T. Fossen, "Maneuvering theory," in *Handbook of Marine Craft Hydrodynamics and Motion Control*, vol. 3, 1st ed. Hoboken, NJ, USA: Wiley, 2011, pp. 133–136.

[21] K. D. Do, Z.-P. Jiang, and J. Pan, "Underactuated ship global tracking under relaxed conditions," *IEEE Trans. Autom. Control*, vol. 47, no. 9, pp. 1529–1536, Sep. 2002.

[22] Y.-X. Li, "Finite time command filtered adaptive fault tolerant control for a class of uncertain nonlinear systems," *Automatica*, vol. 106, pp. 117–123, Aug. 2019.

[23] Y. Ma, G. Zhu, and Z. Li, "Error-driven-based nonlinear feedback recursive design for adaptive NN trajectory tracking control of surface ships with input saturation," *IEEE Intell. Transp. Syst. Mag.*, vol. 11, no. 2, pp. 17–28, Mar. 2019.

[24] C. Wang and Y. Lin, "Decentralized adaptive tracking control for a class of interconnected nonlinear time-varying systems," *Automatica*, vol. 54, pp. 16–24, Apr. 2015.

[25] Q. Zhang, M. Zhang, R. Yang, and N. Im, "Adaptive neural finite-time trajectory tracking control of MSVs subject to uncertainties," *Int. J. Control, Autom. Syst.*, vol. 19, no. 6, pp. 2238–2250, Mar. 2021.

[26] K. Y. Pettersen and O. Egeland, "Exponential stabilization of an underactuated surface vessel," in *Proc. 35th IEEE Conf. Decis. Control*, Dec. 1996, pp. 967–972.

[27] F. Mazenc, K. Pettersen, and H. Nijmeijer, "Global uniform asymptotic stabilization of an underactuated surface vessel," *IEEE Trans. Autom. Control*, vol. 47, no. 10, pp. 1759–1762, Oct. 2002.

[28] W. Dong and Y. Guo, "Global time-varying stabilization of underactuated surface vessel," *IEEE Trans. Autom. Control*, vol. 50, no. 6, pp. 859–864, Jun. 2005.

[29] K. Y. Pettersen and T. I. Fossen, "Underactuated dynamic positioning of a ship-experimental results," *IEEE Trans. Control Syst. Technol.*, vol. 8, no. 5, pp. 856–863, Sep. 2000.

YANG LIU received the M.Sc. degree in traffic information engineering and control from Jimei Maritime University, in 2012. He is currently pursuing the Ph.D. degree with Mokpo Maritime University. His research interests include ship automatic control study, nonlinear feedback control, ship maneuvering simulation and its applications, and marine traffic simulation.

NAM-KYUN IM received the M.Sc. degree in navigation science from Korea Maritime University, in 1992, and the Ph.D. degree in naval architecture and ocean engineering from Osaka University, Japan, in 2002. He was at the Ship and Ocean Research Center of Samsung Heavy Industry around three years. He is currently a Professor with Mokpo National Maritime University. His research interests include ship automatic control study, ship maneuvering simulation and its applications, marine traffic simulation, ship free running model, and marine/ship environmental issues.